DNA double-strand breaks and homology search: inferences from a species with incomplete pairing and synapsis

Adela Calvente[1,*], Alberto Viera[1,*], Jesús Page[1], M. Teresa Parra[1], Rocío Gómez[1], José A. Suja[1], Julio S. Rufas[1,‡] and Juan L. Santos[2]

[1]Departamento de Biología, Facultad de Ciencias, Universidad Autónoma de Madrid, Cantoblanco, 28049 Madrid, Spain
[2]Departamento de Genética, Facultad de Biología, Universidad Complutense de Madrid, 28040 Madrid, Spain
*These authors contributed equally to this work
‡Author for correspondence (e-mail: julio.s.rufas@uam.es)

Accepted 21 March 2005
Journal of Cell Science 118, 2957-2963 Published by The Company of Biologists 2005
doi:10.1242/jcs.02391

Summary

The relationship between meiotic recombination events and different patterns of pairing and synapsis has been analysed in prophase I spermatocytes of the grasshopper *Stethophyma grossum*, which exhibit very unusual meiotic characteristics, namely (1) the three shortest bivalents achieve full synapsis and do not show chiasma localisation; (2) the remaining eight bivalents show restricted synapsis and proximal chiasma localisation, and (3) the X chromosome remains unsynapsed. We have studied by means of immunofluorescence the localisation of the phosphorylated histone H2AX (γ-H2AX), which marks the sites of double-strand breaks; the SMC3 cohesin subunit, which is thought to have a close relationship to the development of the axial element (a synaptonemal complex component); and the recombinase RAD51. We observed a marked nuclear polarization of both the maturation of SMC3 cohesin axis and the ulterior appearance of γ-H2AX and RAD51 foci, these being exclusively restricted to those chromosomal regions that first form cohesin axis stretches. This polarised distribution of recombination events is maintained throughout prophase I over those autosomal regions that are undergoing, or about to undergo, synapsis. We propose that the restricted distribution of recombination events along the chromosomal axes in the spermatocytes is responsible for the incomplete presynaptic homologous alignment and, hence, for the partial synaptonemal complex formation displayed by most bivalents.

Supplementary material available online at
http://jcs.biologists.org/cgi/content/full/118/13/2957/DC1

Key words: Double-strand breaks, Synapsis, Recombination, γ-H2AX, Meiosis, RAD51

Introduction

Meiosis is a specialised type of cell division by which sexually reproducing eukaryotes maintain their chromosome number across generations. In this process, haploid gametes are produced by two successive rounds of chromosome segregation after a single DNA replication round. During first meiotic prophase homologues form stable bivalents, a process which, in most organisms, involves homologous recognition with a subsequent step of intimate alignment (pairing), synapsis (close association of paired chromosomes by synaptonemal complex proteins) and recombination (exchange of chromosomal regions). The physical connections between homologues produced as a consequence of reciprocal recombination events (chiasmata), in combination with sister chromatid arm cohesion, are responsible for the correct bi-orientation of bivalents at metaphase I and the subsequent segregation of a complete set of chromosomes at anaphase I. Sister chromatids separate at the second division generating haploid gametes. Fusion of gametes at fertilisation restores the diploid chromosome number of the species and initiates zygote development.

In some model organisms, the successful pairing of homologous chromosomes depends on the meiotic recombination pathway initiated by programmed double-strand breaks (DSBs) catalysed by SPO11, a topoisomerase-II-like protein (Keeney et al., 1997; Baudat et al., 2000; Romanienko and Camerini-Otero, 2000; Grelon et al., 2001; Peoples et al., 2002). DSB formation requires the products of at least nine other genes that are involved in either stabilisation or recruitment mechanisms (Keeney, 2001). DSBs also induce the phosphorylation of certain variants of the histone H2A, such as H2AX, H2Av (Redon et al., 2002; Madigan et al., 2002) and H2B (Fernández-Capetillo et al., 2004). These modifications are associated with the recruitment of repair factors to damaged DNA in order to facilitate repair efficiency (Madigan et al., 2002; Celeste et al., 2003). DSB ends are degraded from their 5′ end, which gives rise to single-stranded DNA that is thought to be used by recombinases to invade double-stranded DNA and form heteroduplex regions (Haber, 2002). Two major recombinases have been described: RAD51 and its meiosis-specific homolog DMC1, both of which are homologues of the bacterial RecA protein (Bishop et al., 1992; Shinohara et al., 1992; Bishop, 1994). It is well established that RAD51 is involved in both mitotic and meiotic recombination (Shinohara

et al., 1992). By analogy with the functions of the RecA protein, RAD51 is also expected to be involved in homology search, (Ashley et al., 1995; Rockmill et al., 1995; Barlow et al., 1997; Moens et al., 1997) and recent evidence reinforces this suggestion (Franklin et al., 1999; Moens et al., 2002; Pawlowski et al., 2003; Tsubouchi and Roeder, 2003).

For decades, grasshoppers were considered a model organism for studying meiotic pairing and synapsis. Immunocytological studies in the species *Locusta migratoria* and *Eyprepocnemis plorans* on the location of the phosphorylated histone H2AX (γ-H2AX) – which marks sites of DSBs – in combination with the recombinase RAD51 and the cohesin subunit SMC3 have led us to suggest that, at least in the two species analysed, certain steps in the recombination pathway might be required for normal synapsis (Viera et al., 2004a). This sequence of meiotic events also occurs in yeast (reviewed in Kleckner, 1996; Roeder, 1997), mouse and *Arabidopsis thaliana* (Grelon et al., 2001; Mahadevaiah et al., 2001), but not in *Drosophila melanogaster* and *Caenorhabditis elegans* (Derburg et al., 1998; Page and Hawley, 2001).

To obtain a better understanding of the roles of DSBs and RAD51 in the processes of pairing and synapsis, we analysed here the sequence of the chromosomal localisation of γ-H2AX and RAD51 proteins in spermatocytes of the grasshopper *Stethophyma grossum*. This species displays singular meiotic features because there are three different synaptic situations within each spermatocyte: (1) Full synapsis in the three shortest bivalents of the complement, (2) partial synapsis restricted to centromeric ends in the remainder eight bivalents, and (3) the unsynapsed X chromosome (Jones, 1973; Fletcher, 1977; Wallace and Jones, 1978; Jones and Wallace, 1980). Therefore, this bizarre natural system provides the possibility of analysing, within the same nuclear environment, the relationship between recombination events and different patterns of pairing and synapsis.

Materials and Methods

Adult males of *Stethophyma grossum* (Orthoptera; Acrididae) were used for this study. The material was processed using the squash procedure described by Page et al. (Page et al., 1998).

Feulgen-Rossenbeck staining

Testes were fixed in 3:1 ethanol:acetic acid and stored at 4°C until required. The fixed material was hydrated for 15 minutes in distilled water. Afterwards, the seminiferous tubules were immersed in 5N HCl at 20°C for 30-40 minutes, thoroughly washed in distilled water and stained with Schiff reagent (Merck) for at least 30 minutes. Two or three tubules were placed per slide and squashed into a drop of 50% acetic acid.

Antibodies

A polyclonal rabbit anti-SMC3 antibody (AB3914; Chemicon International) raised against a synthetic peptide of human SMC3 was used to detect the cohesin subunit SMC3 at a 1:30 dilution in PBS. It is important to note that only the lot number 220701985 of the antibody works in grasshoppers whereas the actual stock commercialised by Chemicon does not. A monoclonal mouse antibody (number 05-636; Upstate) raised against amino acids 134-142 of human histone γ-H2AX was used to detect the histone variant γ-H2AX (Paull et al., 2000) at a 1:500 dilution in PBS. This peptide sequence is identical in yeast and mouse (Redon et al., 2002). A polyclonal rabbit anti-RAD51 antibody (Ab-1; PC130; Oncogene Research Products), generated against recombinant HsRAD51 protein, was used to detect the recombinase RAD51 at a 1:30 dilution in PBS. All antibodies used in the present study have previously been tested in grasshopper immunoblot assays (Viera et al., 2004a). A monoclonal mouse anti-topoisomerase IIα antibody (MAB4197; Chemicon International) against a major 170 kDa protein (that was identified as the α isoform of human topoisomerase II) was used to detected the topoisomerase IIα protein at 1:5 dilution in PBS.

Immunofluorescence

Fixed spermatocytes were incubated overnight at 4°C with primary antibodies. Following three washes of 5 minutes in PBS, primary antibodies were revealed with the appropriate secondary antibodies conjugated with either FITC or Texas Red (Jackson ImmunoResearch Laboratories) at a 1:150 dilution in PBS, counterstained with 4',6-diamidino-2-phenylindole (DAPI) 10 μg/ml, thoroughly washed in PBS and finally mounted with Vectashield (Vector Laboratories). In double-immunolabelling experiments both primary antibodies were incubated simultaneously, except when they had been generated in the same host species. In this last case, slides were first incubated with the first primary antibody (anti-SMC3) for 1 hour at room temperature, rinsed three times for 5 minutes in PBS and incubated overnight at 4°C with an FITC-conjugated goat Fab′ fragment anti-rabbit IgG (Jackson) at a 1:100 dilution in PBS. Afterwards, slides were rinsed at least six times for 5 minutes in PBS, incubated with the second primary antibody (anti-RAD51) for 1 hour at room temperature, rinsed three times for 5 minutes in PBS and then incubated with a Texas Red-conjugated goat anti-rabbit IgG (Jackson) at a 1:150 dilution. Finally, slides were counterstained with DAPI and mounted as previously described.

Observations were performed using an Olympus BX61 microscope equipped with a motorised *Z*-axis and epifluorescence optics. Stacks of images were captured with a DP70 Olympus digital camera using the AnalySIS software from Olympus and finally analysed and processed using the public domain ImageJ software (National Institutes of Health, USA; http://rsb.info.nih.gov/ij), VirtualDub (http://virtualdub.org/) and Adobe Photoshop 6.0 software.

Results

Bivalents display chiasma localisation in spermatocytes of *Stethophyma grossum*

Feulgen-stained metaphase I spermatocytes allowed us the visualisation of the chromosome complement of this species that consists of eleven autosomal bivalents plus a single sex chromosome. All chromosomes showed terminally located centromeres. Bivalents are usually monochiasmatic although two chiasmata were occasionally observed in the M9 bivalent. Whereas the single chiasma is not restricted to any particular chromosome region in the shortest bivalents (M9-S11), it is located near the centromere in the rest of the bivalents (L1-M8) (see supplementary material Fig. S1). These results concur with previous observations (White, 1936; Perry and Jones, 1974).

DSBs appear at prophase I before synapsis

To establish accurately the sequence of prophase I stages we used an antibody against the SMC3 protein. This protein is a member of the structural maintenance of chromosomes (SMC) family of proteins, which is widespread in eukaryotes (Hirano,

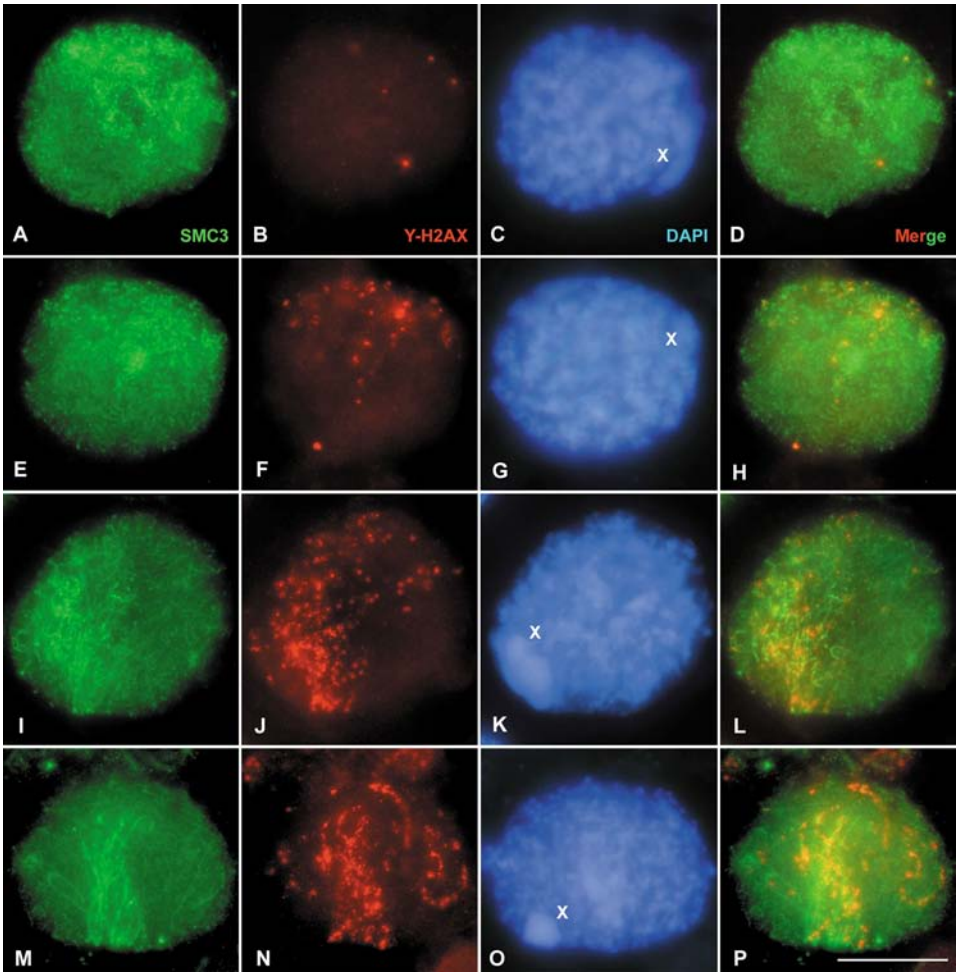

Fig. 1. Meiotic γ-H2AX foci encompass cohesin-axis assembly. Early stages of male meiosis after double immunolabelling for the cohesin subunit SMC3 (green in first column) and the histone variant γ-H2AX (red in second column). Merged images (SMC3 and γ-H2AX) are presented in the forth column. The third column shows chromatin organisation (DAPI staining, blue). All images correspond to the accumulative superimposition of several focal planes. A progressive increase in the cohesin-axis maturation and the number of γ-H2AX foci can be detected. (A-D) Pre-leptotene. Short SMC3 stretches are detected in a discrete nuclear region (A). Few γ-H2AX foci (B) are located on these SMC3 threads (D). From early (E-H) up to late (I-L) leptotene, the maturation and linear organisation of the axes occur concomitantly with an increase of γ-H2AX foci. All γ-H2AX foci are located over the cohesin axes. (M-P) Zygotene spermatocyte characterised by the presence of parallel thick SMC3 threads located at a discrete region of the nucleus, denoting a bouquet-like organisation. Notice that in these stages no γ-H2AX staining is detected on the sex chromosome (X). Bar, 10 μm.

2002). SMC3 is involved in sister chromatid cohesion during meiosis, and also seems to be essential for the organisation of an axial element (AE) structure in which chromatin loops are attached in mammal meiosis (Eijpe et al., 2000; Pelttari et al., 2001; James et al., 2002). In grasshoppers, the AE development has been analysed indirectly at prophase I by an antibody against SMC3. Although it was not possible to assay the synaptonemal complex (SC) formation directly, it could be inferred from the identification of thick and thin SMC3 filaments, which correspond to synapsed and unsynapsed regions, respectively (Viera et al., 2004a) (see also supplementary material Movie 1). On these grounds, we assume that in *Stethophyma grossum* the SMC3 immunolocalisation patterns reflect the different stages of synaptic development that can be related to the sequence of appearance of γ-H2AX and RAD51 proteins throughout prophase I.

The pre-leptotene stage was characterised by SMC3 dot-like labelling along the entire nucleus (Fig. 1A). At that time, the first γ-H2AX foci, corresponding to the occurrence of DSBs, were observed (Fig. 1B). These few foci were associated to the initial threads of cohesin axis signals (Fig. 1D, supplementary material Movie 2). The SMC3 labelling, observed from early to late leptotene, appears as well-defined linear stretches longer than those observed at pre-leptotene (Fig. 1E,I). Concomitantly, the number of γ-H2AX foci increased rapidly (Fig. 1F,J), being massively concentrated over the recently formed SMC3 cohesin axes (Fig. 1H,L). Surprisingly, the sequence of cohesin axis formation occurred in defined regions of the nuclei throughout leptotene. Whereas cohesin axes were first formed and elongated in a determined nuclear region, the rest of the nucleus maintained the pre-leptotene dot-like appearance (Fig. 1I). It is worth mentioning that the formation of DSBs appeared to be restricted and polarised at the nuclear region in which the cohesin axis formation was advanced (Fig. 1H,L). Observations of cohesin axis positioning did not reveal any evidence of homologous alignment.

In zygotene spermatocytes the SMC3 cohesin axis maturation increased and appeared as well-defined thin lines all over the nucleus. Interestingly, paired cohesin axes that form thick filaments (synapsed regions) were only concentrated over a determined nuclear region that resembled a ‘bouquet-like’ arrangement (Fig. 1M). By contrast, the unsynapsed autosomal regions remained dispersed in the nucleus and are not associated in pairs (Fig. 1M). At zygotene, γ-H2AX was detected as ribbons (Fig. 1N) associated with the chromatin adjacent to autosomal regions that had undergone, or were undergoing, pairing and synapsis. At these regions, SMC3 axes displayed parallel trajectories to each other. However, the chromosomal regions in which pairing was never to be completed showed irregular SMC3 axis trajectories and no γ-H2AX labelling (Fig, 1P). From mid-zygotene to pachytene γ-H2AX signalling started to disappear (compare Fig. 1N and Fig. 2B).

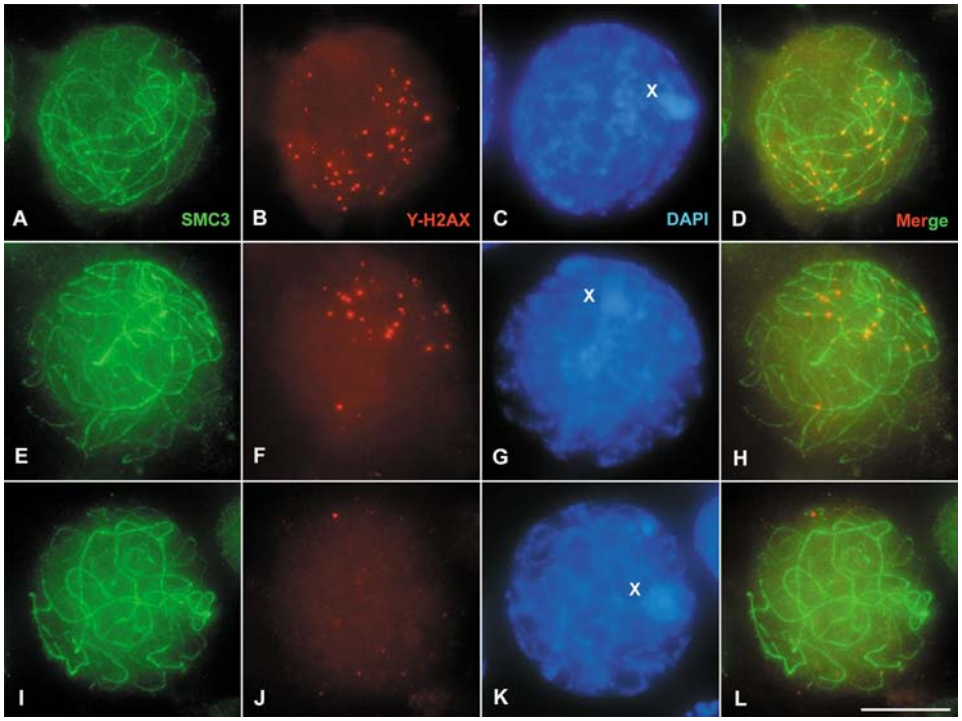

Fig. 2. Discrete γ-H2AX foci are located over synapsed autosomal regions at pachytene. Three different pachytene spermatocytes after double immunolabelling of the cohesin subunit SMC3 (green) and the histone variant γ-H2AX (red). Merged images (SMC3 and γ-H2AX, fourth column) and DAPI stained nuclei (blue) are also shown. SMC3 staining indicates the absence of full synapsis (A,E,I). The number of γ-H2AX foci reveals the different pachytene substages. Early pachytene (A-D) with a large amount of γ-H2AX foci. The number of foci varies from seven to 12 in mid-pachytene (E-H), but foci are absent in late pachytene (I-L). Notice that the amount of synapsis is similar in all pachytene sub-stages. X indicates sex chromosome. Bar, 10 μm.

Surprisingly, pachytene spermatocytes maintained the marked nuclear polarisation of the cohesin-axis maturation and the synaptic state of homologues observed at zygotene (Fig. 2A,E,I). Therefore, throughout all pachytene sub-stages and within the same nucleus we found bivalents that achieved full synapsis, bivalents with incomplete synapsis (from one of their ends to almost half of their lengths) and the unsynapsed X chromosome. These results reinforced previous observations on the existence of partial synapsis in the spermatocytes of this species (Fletcher, 1977; Wallace and Jones, 1978; Jones and Wallace, 1980). At pachytene, γ-H2AX labelling also appeared polarised and reduced to a few discrete foci (Fig. 2B,F,J), which were located over the autosomal synapsed regions (Fig. 2D,H,L and supplementary material Movie 3). The number of γ-H2AX foci found at early pachytene (Fig. 2B) decreased by mid-pachytene (Fig. 2F) and was almost absent at late pachytene (Fig. 2J). γ-H2AX was not observed until the formation of spermatids (data not shown). Spermatid labelling has previously been reported in mouse (Hamer et al., 2003) and in two species of grasshoppers (Viera et al., 2004a). Therefore, our results indicate that, in *Stethophyma grossum* spermatocytes, extensive DSBs formation occurs before pairing and is strictly restricted to those autosomal regions that undergo synapsis (compare with the prophase I sequence of these events in the standard grasshopper species *Eyprepocnemis plorans*, see supplementary material Figs S2 and S3).

γ-H2AX is absent from the single X chromosome

The single X chromosome usually occupied a peripheral zone of the nucleus during prophase I (X in Fig. 1C,G,K,O and Fig. 2C,G,K). No SMC3 signalling was detectable in the X chromosomes until late leptotene, when its cohesin axis became evident (compare Fig. 1A,C,E,G with I,K). Therefore, the pattern of conformation and maturation of the cohesin axis in the X chromosome was delayed compared with that in autosomes. Throughout prophase I, the X chromosome remained unsynapsed and without any signs of γ-H2AX labelling, even though it was preferentially embedded in the nuclear domain, which contained the autosomal synapsed regions encompassed with strong γ-H2AX staining (Figs 1 and 2).

Unsynapsed chromosomal regions are devoid of RAD51 foci

RAD51 first appeared as few discrete foci on the incipient stretches of autosomal cohesin axes at early leptotene (Fig. 3A,B,D). During leptotene, the number of RAD51 foci increased dramatically but foci were restricted to the polarised nuclear domain in which the cohesin axis formation was advanced (Fig. 3E,F,H). The rest of the nucleus, showing cohesin axes in a pre-leptotene-like appearance, was devoid of RAD51 foci (Fig. 3H). At zygotene, RAD51 foci were polarised on a nuclear domain (Fig. 3J), being closely associated to the synapsed or almost synapsed autosomal regions that displayed the 'bouquet-like' rearrangement (Fig. 3L). However, we did not detect RAD51 foci within the unsynapsed chromosomal regions that dispersedly occupied the rest of the nucleus (Fig. 3I-L). From early to mid-pachytene spermatocytes (Fig. 3M-T), the number of RAD51 foci decreased until they had disappeared completely in late pachytene nuclei. Notice that, whereas RAD51 labelling was never associated with the single X chromosome (X in Fig. 3C,G,K,O,S), the γ-H2AX labelling was.

Double immunolabelling of spermatocytes with anti-γ-H2AX and anti-RAD51 antibodies are shown in the supplementary material (Fig. S4). γ-H2AX histone appeared earlier in pre-leptotene and at this stage no RAD51 foci were

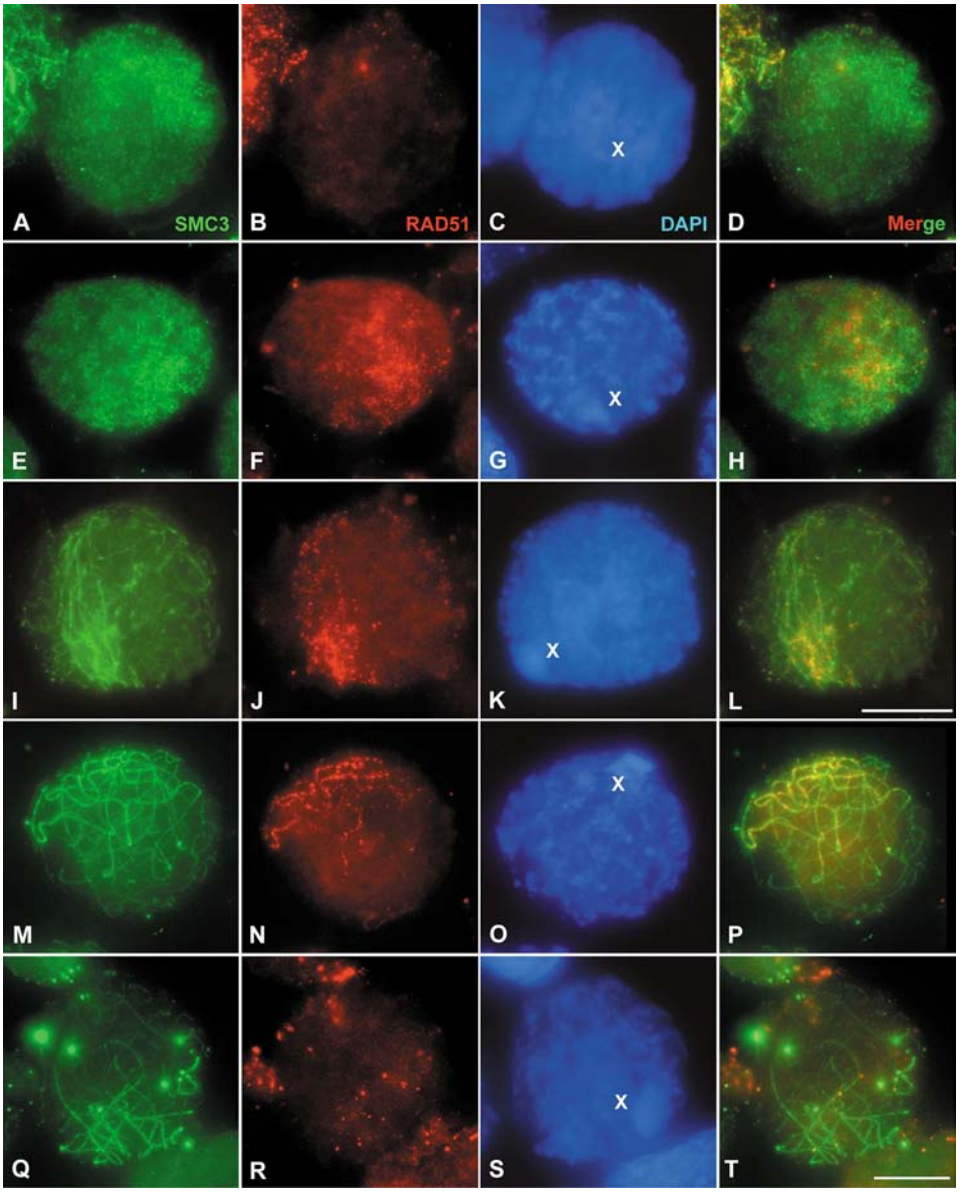

Fig. 3. RAD51 foci appear over cohesin axes. Early meiotic stages of male meiosis after double immunololabelling of the cohesin subunit SMC3 (green in first column) and the recombinase RAD51 (red in second column). Merged images (SMC3 and γ-H2AX) are in the forth column and DAPI stained nuclei (blue) are observed in the third one. Several focal planes were merged to obtain each image. Early leptotene (A-D) is characterised by the presence of threads of cohesin axes in a polarised nuclear region (A). Notice that RAD51 foci (B) are located over SMC3 threads (D). Mid-leptotene (E-H). Progressive maturation of cohesin axes (E). The number of RAD51 foci rapidly increase (F) and remain associated to the cohesin axes (H). The characteristic bouquet-like arrangement can be identified in zygotene spermatocytes (I-L). Both SMC3 paired-axes (I) and RAD51 foci (J) are polarised in a discrete region of the nucleus. It is evident that the localisation of RAD51 foci is strictly restricted to paired cohesin axes (L). RAD51 foci are restricted to thick, synapsed, cohesin axes at early pachytene (M-P). Mid-pachytene (Q-T) shows a lower amount of RAD51 foci (R). Notice that, in all cases RAD51 signals are located over synapsed regions (D,H,L,P,T). X indicates sex chromosome. Bars, 10 μm.

detected. At leptotene the initial RAD51 foci were associated with the γ-H2AX signals. At zygotene, the strong γ-H2AX staining was surrounded by a large number of RAD51 foci that were located within the γ-H2AX ribbons. At pachytene, both RAD51 and γ-H2AX signals were reduced to a few discrete foci. From late pachytene onwards, neither γ-H2AX nor RAD51 were detectable.

Discussion

Our results on the relative order of DSBs formation in spermatocytes of *Stethophyma grossum*, based on the appearance and distribution of γ-H2AX and RAD51, indicated that γ-H2AX immunostaining occurs at early leptotene when only short stretches of SMC3 cohesin axes are formed. Since direct evidence has pointed towards a relationship between cohesin axis maturation and the assembly of AEs (Revenkova et al., 2004), our observations on SMC3 cohesin axis maturation might reflect the AE morphogenesis and, therefore, the processes of SC assembly. In this sense, our results demonstrate that, in this species, the initiation of recombination events, detected by γ-H2AX labelling, occurs before synapsis is initiated and thus in the absence of a tripartite SC structure. Additionally, we observed that RAD51 foci appeared immediately after γ-H2AX-labelling and, therefore, downstream of DSBs formation. Similar results have recently been reported in two other grasshopper species although in those cases DSBs formation occurred at the leptotene-zygotene transition (Viera et al., 2004a). These situations concur with the recombination pathway that has been described in budding yeast (reviewed in Kleckner, 1996; Roeder, 1997), mouse (Mahadevaiah et al., 2001) and *Arabidopsis* (Grelon et al., 2001). Intriguingly, recombination events in spermatocytes of *Stethophyma grossum* are not equally distributed within the whole nuclear chromatin, as described for all other organisms studied to date (reviewed in Zickler and Kleckner, 1999). Indeed, recombination events are exclusively polarised and restricted to a certain nuclear domain, occupied by those autosomal regions that are undergoing or are about to undergo synapsis. It is tempting to speculate that the polarised distribution of γ-H2AX and RAD51 is conditioned by the preceding nuclear polarisation of the morphogenesis and maturation of the cohesin axis, which is perhaps also

associated with conformational changes in the chromatin (Prieto et al., 2004). Previous studies on *Stethophyma grossum* spermatocytes have demonstrated that only the shortest bivalents – M9, S10 and S11 – can achieve full synapsis, whereas in the remaining bivalents, L1-M8, synapsis is restricted to their centromeric regions and about half their lengths (Wallace and Jones, 1978). Consequently, we can assume that by early leptotene the shortest bivalents and the regions close to the centromeres of the L1-M8 bivalents are mainly localised in the nuclear domain in which cohesin axis formation and maturation is more advanced. During leptotene, recombination machinery would immediately be recruited only to autosomal regions that present an advanced cohesin axis-AE morphogenesis; even they still do not show evidence of homologous alignment. Afterwards, only chromosomal regions with previously developed cohesin axes will be able to achieve pairing and synapsis, whereas the X chromosome and the non-centromeric regions of L1-M8 bivalents that lack DSBs and RAD51 foci will not. A similar pattern has also been described for grasshopper accessory-chromosomes when they remain univalent throughout meiosis (Viera et al., 2004b). Moreover, DSB-dependent but SC-independent homologous alignment has also been reported in budding yeast (Peoples et al., 2002) and the fungus *Sordaria macrospora* (Tessé et al., 2003). Additionally, direct evidence of a link between recombination and chromosome pairing has arisen from observations in maize meiotic mutants, in which a correlation has been found between significant decreases in the number of RAD51 foci at zygotene and the degree of their pairing defects (Pawlowski et al., 2003). Likewise, the *rad51-1* mutant of *Arabidopsis* exhibits a failure in chromosome pairing and synapsis (Li et al., 2004). Although RAD51-mediated homology search seems to be crucial for pairing and synapsis in organisms as different as yeast, mice, plants and grasshoppers, the situation is different in other species. For instance, a *C. elegans RAD51* knockout resulted in abnormal chromosomal morphology and univalent formation at diakinesis but did not affect meiotic homology recognition and synapsis (Alpi et al., 2003).

In *Stethophyma grossum* spermatocytes only one (occasionally two, in M9) of all recombination events observed per bivalent lead to crossover-formation that manifested itself as a chiasma. Fully synapsed M9, S10 and S11 bivalents did not present chiasma localisation at metaphase I, whereas the longest bivalents (L1-M8), which presented incomplete pairing and synapsis, always displayed chiasma localisation. In some L1-M8 bivalents, chiasmata form very close to the centromere and in other ones they form at some distance from the centromere, but in no case does the centromere to chiasma distance exceed the length of the S11 chromosome (Perry and Jones, 1974; see also supplementary material Fig. S1). Moreover, it was observed that only a region comparable in length to the S11 bivalent is paired and synapsed in each of the longest bivalents (Wallace and Jones, 1978; and this work). Thus, large bivalents would only produce a single crossover because they behave like shorts ones in respect of generating crossovers and the corresponding interference signalling along their length. Accordingly, the formation of a second chiasma in L1-M8 bivalents would be prevented because of a strict regulation of interference signals that can be transmitted either along chromosomal axes (Börner et al., 2004) (reviewed by Bishop and Zickler, 2004) or through the SC (reviewed by Sinohara et al., 2003). Notice that, in contrast to males, chiasmata are not localised in females of *Stethophyma grossum* (Perry and Jones, 1974). The evolutionary reason for these differences between the sexes remains to be ascertained and further studies are necessary to investigate them.

This work was supported by grants BMC2002-0043 and BMC2002-1171 from Ministerio de Ciencia y Tecnología (Spain). A. C. has a predoctoral fellowship from Fundación General de la Universidad Autónoma de Madrid and Olympus Optical España S.A. R.G. has a predoctoral fellowship from Universidad Autónoma de Madrid and Fundación Francisco Cobos.

References

Alpi, A., Pasierbek, P., Gartner, A. and Loidl, J. (2003). Genetic and cytological characterization of the recombination protein RAD-51 in *Caenorhabditis elegans. Chromosoma* **112**, 6-16.

Ashley, T., Plug, A. W., Xu, J., Solari, A. J., Reddy, G., Golub, E. I. and Ward, D. C. (1995). Dynamic changes in Rad51 distribution on chromatin during meiosis in male and female vertebrates. *Chromosoma* **104**, 19-28.

Barlow, E. L., Benson, F. E., West, S. C. and Hultén, M. A. (1997). Distribution of the Rad51 recombinase in human and mouse spermatocytes. *EMBO J.* **16**, 5207-5215.

Baudat, F., Manova, K., Yuen, J. P., Jasin, M. and Keeney, S. (2000). Chromosome synapsis defects and sexually dimorphic meiotic progression in mice lacking Spo11. *Mol. Cell.* **6**, 989-998.

Bishop, D. K. (1994). RecA homologs Dmc1 and Rad51 interact to form multiple nuclear complexes prior to meiotic chromosome synapsis. *Cell* **79**, 1081-1092.

Bishop, D. K. and Zickler, D. (2004). Early decision; meiotic crossover interference prior to stable strand exchange and synapsis. *Cell* **117**, 9-15.

Bishop, D. K., Park, D., Xu, L. and Kleckner, N. (1992). *DMC1*: A meiosis-specific yeast homolog of *E. coli* recA required for recombination, synaptonemal complex formation, and cell cycle progression. *Cell* **69**, 439-456.

Börner, G. V., Kleckner, N. and Hunter, N. (2004). Crossover/noncrossover differentiation, synaptonemal complex formation, and regulatory surveillance at the leptotene/zygotene transition of meiosis. *Cell* **117**, 29-45.

Celeste, A., Fernández-Capetillo, O., Kruhlak, M. J., Pilch, D. R., Staudt, A., Lee, D. W., Bonner, R. F., Bonner, W. M. and Nussenzweig, A. (2003). Histone H2AX phosphorylation is dispensable for the initial recognition of DNA breaks. *Nat. Cell Biol.* **5**, 675-679.

Dernburg, A. F., McDonald, K., Moulder, G., Barstead, G., Dresser, M. and Villeneuve, A. M. (1998). Meiotic recombination in *C. elegans* initiates by a conserved mechanism and is dispensable for homologous chromosome synapsis. *Cell* **94**, 387-398.

Eijpe, M., Heyting, C., Gross, B. and Jessberger, R. (2000). Association of mammalian SMC1 and SMC3 proteins with meiotic chromosomes and synaptonemal complexes. *J. Cell Sci.* **113**, 673-682.

Fernández-Capetillo, O., Allis, C. D. and Nussenzweig, A. (2004). Phosphorylation of histone H2B at DNA double-strand breaks. *J. Exp. Med.* **199**, 1671-1677.

Fletcher, H. L. (1977). Localised chiasmata due to partial pairing: a 3D reconstruction of synaptonemal complexes in male *Stethophyma grossum*. *Chromosoma* **65**, 247-269.

Franklin, A. E., McElver, J., Sunjevaric, I., Rothstein, R., Bowen, B. and Cande, W. Z. (1999). Three-dimensional microscopy of Rad51 recombination protein during meiotic prophase. *Plant Cell* **11**, 809-824.

Grelon, M., Vezon, D., Gendrot, G. and Pelletier, G. (2001). At *SPO11-1* is necessary for meiotic recombination in plants. *EMBO J.* **20**, 589-600.

Haber, J. E. (2000). Partner and pathways repairing a double-strand break. *Trends Genet.* **6**, 259-264.

Hamer, G., Roepers-Gajadien, L. P., van Duyn-Goedhart, A., Gademan, I. S., Kal van, H. B., Buul, P. P. W. and de Rooij, D. G. (2003). DNA double-strand breaks and γ-H2AX signalling in the testis. *Biol. Reprod.* **68**, 628-634.

Hirano, T. (2002). The ABCs of SMC proteins: two-armed ATPases for chromosome condensation, cohesion, and repair. *Genes Dev.* **16**, 399-414.

James, D. R., Schmiesding, J. A., Peters, A. H. F. M., Yokomori, K. and

Disteche, C. M. (2002). Differential association of SMC1α and SMC3 proteins with meiotic chromosomes in wild-type and SPO11-deficient male mice. *Chromosome Res.* **10**, 549-560.

Jones, G. H. (1973). Light and electron microscope studies of chromosome pairing in relation to chiasma localisation in *Stethophyma grossum* (Orthoptera: Acrididae). *Chromosoma* **42**, 145-162.

Jones, G. H. and Wallace, B. M. N. (1980). Meiotic chromosome pairing in *Stethophyma grossum* spermatocytes studied by a surface-spreading and silver-staining technique. *Chromosoma* **78**, 189-201.

Keeney, S. (2001). Mechanism and control of meiotic recombination initation. *Curr. Top. Dev. Biol*. **52**, 1-53.

Keeney, S., Giroux, C. N. and Kleckner, N. (1997). Meiosis–specific DNA double-strand breaks are catalysed by Spo11, a member of a widely conserved protein family. *Cell* **88**, 375-384.

Kleckner, N. (1996). Meiosis: how could it work? *Proc. Natl. Acad. Sci. USA* **93**, 8167-8174.

Li, W., Chen, C., Markmann-Mulisch, U., Timofejeva, L., Schmelzer, E., Ma, H. and Reiss, B. (2004). The Arabidopsis *AtRAD51* gene is dispensable for vegetative development but required for meiosis. *Proc. Natl. Acad. Sci. USA* **101**, 10596-10601.

Madigan, J. P., Chotkoswski, H. L. and Glaser, R. L. (2002). DNA double-strand break-induced phosphorylation of *Drosophila* histone variant H2Av helps prevent radiation-induced apoptosis. *Nucleic Acids Res.* **30**, 3698-3705.

Mahadevaiah, S. K., Turner, J. M., Baudat, F., de Rogaku, E. P., Boer, P., Blanco-Rodriguez, J., Jasin, M., Keeney, S., Bonner, W. M. and Burgoyne. P. S. (2001). Recombinational DNA double strand breaks in mice precede synapsis. *Nat. Genet*. **21**, 271-276.

Moens, P. B., Chen, D. J., Shen, Z., Kolas, N., Tarsounas, M., Heng, H. H. Q. and Spyropoulos, B. (1997). Rad51 immunocytology in rat and mouse spermatocytes and oocytes. *Chromosoma* **106**, 207-215.

Moens, P. B., Kolas, N. K., Tarsounas, M., Marcon, E., Cohen, P. E. and Spyropoulos, B. (2002). The time course and chromosomal localisation of recombination-related proteins at meiosis in the mouse are compatible with models that can resolve the early DNA-DNA interactions without reciprocal recombination. *J. Cell Sci*. **115**, 1611-1622.

Page, J., Suja, J. A., Santos, J. L. and Rufas, J. S. (1998). Squash procedure for protein immunolocalisation in meiotic cells. *Chromosome Res*. **6**, 639-642.

Page, S. L. and Hawley. R. S. (2001). c(3)G encodes a *Drosophila* synaptonemal complex protein. *Genes Dev*. **15**, 3130-3143.

Paull, T. T., Rogakou, E. P., Yamazaki, V., Kirchgessner, C. U., Gellert, M. and Bonner, W. M. (2000). A critical role for histone H2AX in recruitment of repair factors to nuclear foci after DNA damage. *Curr. Biol*. **10**, 886-895.

Pawlowski, W. P., Golubovskaya, I. N. and Cande, W. Z. (2003). Altered nuclear distribution of recombination protein RAD51 in maize mutants suggests the involvement of RAD51 in meiotic homology recognition. *Plant Cell* **15**, 1807-1816.

Pelttari, J., Hoja, M.-R., Yuan, L., Liu, J. G., Brundell, E., Moens, P., Santucci-Darmanin, S., Jessberger, R., Barbero, J. L., Heyting, C. et al. (2001). A meiotic chromosome core consisting of cohesin complex proteins recruits DNA recombination proteins and promotes synapsis in the absence of an AE in mammalian meiotic cells. *Mol. Cell. Biol*. **21**, 5667-5677.

Peoples, T. L., Dean, E., González, O., Lambourne, L. and Burgess, S. H. (2002). Close, stable homolog juxtaposition during meiosis in budding yeast is dependent on meiotic recombination, occurs independently of synapsis, and is distinct from DSB-independent pairing contacts. *Genes Dev*. **16**, 1682-1695.

Perry, P. E. and Jones, G. H. (1974). Male and female meiosis in grasshoppers. I. *Stethophyma grossum*. *Chromosoma* **47**, 227-236.

Prieto, P., Shaw, P. and Moore, G. (2004). Homologue recognition during meiosis is associated with a change in chromatin conformation. *Nat. Cell Biol*. **6**, 906-908.

Redon, C., Pilch, D., Rogakou, E. P., Sedelnikova, O., Newrock, K. and Bonner, W. M. (2002). Histone H2A variants H2AX and H2AZ. *Curr. Opin. Genet. Dev*. **12**, 162-169.

Revenkova, E., Ejipe, M., Heyting, C., Hodges, C. A., Hunt, P. A., Liebe, B., Scherthan, H. and Jesseberger, R. (2004). Cohesin SMC1 β is required for meiotic chromosome dynamics, sister chromatid cohesion and DNA recombination. *Nat. Cell Biol.* **6**, 555-562.

Rockmill, B., Sym, M., Scherthan, H. and Roeder, G. S. (1995). Roles for two RecA homologous in promoting meiotic chromosome synapsis. *Genes Dev*. **9**, 2684-2695.

Roeder, G. S. (1997). Meiotic chromosomes: it takes two to tango. *Genes Dev*. **11**, 2600-2621.

Romanienko, P. J. and Camerini-Otero, R. D. (2000). The mouse *Spo11* gene is required for meiotic chromosome synapsis. *Mol. Cell*. **6**, 978-987.

Shinohara, A., Ogawa, H. and Ogawa, T. (1992). Rad51 protein involved in repair and recombination in *Saccharomyces cerevisiae* is a RecA-like protein. *Cell* **69**, 457-470.

Shinohara, M., Sakai, K., Shinohara, A. and Bishop. D. K. (2003). Crossover interference in *Saccharomyces cerevisiae* requires a TID1/RDH54- and DMC1-dependent pathway. *Genetics* **163**, 1273-1286.

Tesse, S., Storlazzi, A., Kleckner, N., Gargano, S. and Zickler, D. (2003). Localisation and roles of Ski8p protein in *Sordaria* meiosis and delineation of three mechanistically distinct steps of meiotic homolog juxtaposition. *Proc. Natl. Acad. Sci. USA* **100**, 12865-1270.

Tsubouchi, H. and Roeder, G. S. (2003). The importance of genetic recombination for fidelity of chromosome pairing in meiosis. *Dev. Cell* **5**, 915-925.

Viera, A., Santos, J. L., Page, J., Parra, M. T., Calvente, A., Cifuentes, M., Gómez, R., Lira, R., Suja, J. A. and Rufas, J. S. (2004a). DNA double-strand breaks, recombination and synapsis: the timing of meiosis differs in grasshoppers and flies. *EMBO Rep*. **5**, 385-391.

Viera, A., Calvente, A., Page, J., Parra, M. T., Gómez, R., Suja, J. A., Rufas, J. S. and Santos, J. L. (2004b). X and B chromosomes display similar meiotic characteristics in male grasshoppers. *Cytogenet. Genome Res*. **106**, 302-308.

Wallace, B. M. N. and Jones, G. H. (1978). Incomplete chromosome pairing and its relation to chiasma localisation in *Stethophyma grossum* spermatocytes. *Heredity* **40**, 385-396.

White, M. J. D. (1936). Chiasma localisation in *Mecostethus grossus* L. and *Metrioptera brachyptera* L. (Orthoptera). *Z. Zellforsch*. **24**, 128-135.

Zickler, D. and Kleckner, N. (1999). Meiotic chromosomes: integrating structure and function. *Annu. Rev. Genet*. **33**, 603-754.